to the *universal stage*, a device that allows rotation of the slide in three dimensions. This is rarely done these days.

Orientation studies are completed by assigning specific axes of the indicatrix to specific crystallographic axes. The identification of the principal axes of the indicatrix is easy. For example, in uniaxial cases, sections showing maximum birefringence contain the unique crystallographic axis, which is parallel to the n_e direction. Knowledge of the optic sign shows which of the two vibration directions coincides with n_e, on the basis of being fast or slow. In biaxial cases, the maximum birefringence section has n_α and n_γ lying in the plane of the slide, and of these n_γ corresponds of course to the slow ray. In biaxial crystals, the identification of the optic axial plane direction in a figure enables immediate identification of the n_β direction, which is normal to it.

1.6.4.15. *Absorption colours*

Many crystalline substances are coloured in transmitted light under the microscope, as a result of the absorption of certain visible-light wave bands. Though there may be much variability between one sample of a substance and another, colour is nevertheless often a great aid in identification.

Absorption, like other optical phenomena, is capable of showing marked anisotropy, the phenomenon known as pleochroism. Pleochroism is usually obvious in both grain mounts and thin sections, because grains change colour when rotated in plane-polarized light. The effect can be subtle (*e.g.* the mineral hypersthene is almost colourless in thin sections but often shows pleochroism from a very faint pink to a very faint green), or very marked (*e.g.* dark brown to colourless or pale yellow in the mineral biotite). The full description of pleochroism involves the assigning of different colours to specific axes of the indicatrix. Uniaxial crystals are *dichroic*, that is, two colours describe the effects. Sections showing centred optic axis figures do not exhibit pleochroism, showing only the pure absorption colours of light vibrating normal to the optic axis (n_o). In biotite for example (which is for practical purposes uniaxial), this colour is usually dark brown. Maximum birefringence sections, or those showing centred flash figures in grain mounts, show maximum pleochroism, one vibration direction exhibiting the n_o absorption already noted, and the other the pure effects of absorption on n_e (in the case of biotite, colourless to pale yellow). Random sections show less pleochroism, and colours that are combinations of the pure end members.

Biaxial crystals can be notably trichroic, and colours are readily assigned by looking at maximum birefringence (flash figure) sections to obtain n_α (fast ray) and n_γ (slow ray) absorptions, and optic axis sections to obtain that for n_β.

The other notable thing about absorption colours is that they can occasionally severely mask polarization colours. Once this is appreciated, the use of the sensitive-tint plate is often sufficient to identify the latter.

1.6.4.16. *Dispersion*

Dispersion, that is to say variation of refractive index depending on wavelength, is a common phenomenon in crystals, and occasionally an important aid in identification. In extreme cases, it results in the production of highly anomalous polarization colours, often browns, blue greys or brownish purples, or bright colours which just look slightly unusual compared with normal second- or third-order colours. Anomalous colours are highly diagnostic of certain substances (*e.g.* the minerals chlorite, zoisite and epidote).

Dispersion also results in a lack of definition of extinction positions, because in biaxial crystals there may effectively be differently oriented indicatrices for different wavelengths. In extreme cases, it may be impossible to locate the extinction position with any accuracy. As an example of a milder case, the very common mineral plagioclase (triclinic) shows subtle, though highly characteristic, features between crossed polars in sections cut approximately normal to the b crystallographic axis. The normal polarization colours seen in between the extinction positions are pure first-order greys and whites, but as a grain is rotated slowly through an extinction position the colours darken and take on a bluish (cold) tinge before going black, and then lighten again with a yellowish (warm) tinge. This is the result of a slight mismatch of the orientations of the indicatrices for long and short wavelengths.

Such dispersion is also often obvious (at least, when looked for) in the interference figures of biaxial crystals. Isogyres become edged with 'cold' (*i.e.* bluish) and 'warm' (tending to red or orange) fringes on opposite sides, indicating that optic axes for different wavelengths have slightly different positions.

Dispersion is a difficult phenomenon to investigate fully with the polarizing microscope. In cubic crystals, it can only be studied systematically by the determination of refractive indices using a number of monochromatic light sources of different wavelengths. Uniaxial crystals can show anomalous polarization colours, but they do not show fringes in interference figures, nor vagueness in extinction position, because the indicatrices for different wavelengths all have the same orientation. Like cubic crystals, however, the dispersion can be investigated by monochromatic light studies of refractive index. Biaxial crystals present the most complex cases. Not only can the shape of the indicatrix vary with wavelength (*i.e.* the relative values of the principal refractive indices), but so can orientation relative to the crystallographic axes. There are even substances known (admittedly with small $2V$) in which the optic axial plane for red light is at right angles to the optic axial plane for violet light. The phenomenon is known as 'crossed axial plane dispersion', a real challenge for the microscopist.

1.6.5. Optical rotation

1.6.5.1. *Introduction*

Optical rotation or gyration, as it is sometimes known, was first recorded by Arago in 1811. Since then, a great deal of work has been done to try to explain this phenomenon, and at the present time it is one of the few physical properties of a crystal that can be successfully understood in terms of the underlying crystal structure (Glazer & Stadnicka, 1986). Lowry (1935) has given a good historical account of the subject.

Optical rotation is the phenomenon observed in some crystals (and in some solutions of, usually, organic compounds) of the rotation of plane-polarized light on passing through the crystal. If the rotation, as seen by the observer, is to the left or counterclockwise it is known as *laevorotation*; if to the right or clockwise it is known as *dextrorotation*. A crystal that shows this effect is sometimes called *optically active* or *gyrotropic*. It is therefore clear that, from a symmetry point of view, optical rotation can only occur in a crystal in which one direction is not equivalent to its opposite, *i.e.* there are no inversion symmetry operations that can change chirality.

One of the earliest theories to explain the origin of optical rotation was given by Fresnel. This was based on the idea that a plane-polarized wave can be equally described by two opposing circularly polarized waves propagating along the same direction. In Fig. 1.6.5.1(*a*), the polarization vector **OA** is simply given by the vector sum of **OB** and **OC**, polarization vectors at some instant of time belonging to a right-circular and a left-circular wave, respectively. Here it is assumed that the light propagates in a direction towards the viewer. If the light now passes through a gyrotropic material, one of the circularly polarized waves will be slowed down with respect to the other (this corresponds to having a small difference in refractive indices for the two waves). Thus on emerging from the crystal, there will be a phase difference between the circular waves, so that on recombining, the resulting

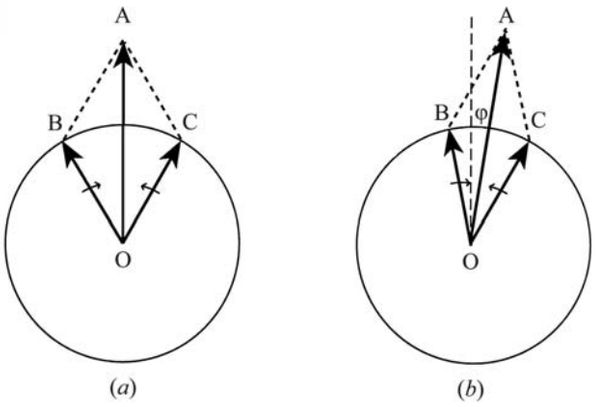

Fig. 1.6.5.1. Fresnel's explanation of optical rotation.

plane of linear polarization **OA** will have rotated through an angle φ. This is shown in Fig. 1.6.5.1(b), where the right-circular (*clockwise*) component travels faster than the left-circular (*anticlockwise*) component. Because of this, in a given time, the electric vector for the right-circular wave, observed in a fixed plane perpendicular to the line of sight, will have rotated through a larger angle clockwise than the electric vector for the left-circular wave will have rotated anticlockwise. The result is a net rotation to the right, *i.e.* dextrorotation, of the vector **OA**. The left and right-circular refractive indices, n_L and n_R, are inversely related to the velocities of the waves, and so Fig. 1.6.5.1(b) corresponds to the case where $n_L > n_R$. Thus this theory shows that a positive value of $n_L - n_R$ defines dextrorotation and that optical rotation is in fact a form of *circular birefringence*.

Fig. 1.6.5.2 illustrates in a more generalized way the nature of the birefringences possible in a crystal. Formally, the refractive index of a medium can be written in terms of real and imaginary components:

$$n = n' + in'', \tag{1.6.5.1}$$

the imaginary component referring to the absorption of the light (the real and imaginary terms are related as usual by the Kramers–Kronig relationship). Similarly, the linear and circular birefringences can also be written in real and imaginary terms:

$$\begin{aligned} \Delta n_{\text{linear}} &= (n_1 - n_2)' + i(n_1 - n_2)'' \\ \Delta n_{\text{circular}} &= (n_L - n_R)' + i(n_L - n_R)''. \end{aligned} \tag{1.6.5.2}$$

The real linear birefringence (a) shows a resonance, changing sign, at a particular wavelength. Its variation with wavelength is known as *birefringent dispersion*. The imaginary component (b) peaks at this wavelength and corresponds to the difference in absorption between linear polarization states. This is called *linear dichroism* (LD) and is determined by quantum-mechanical selection rules resulting from matrix elements of the type $\langle \Psi_1 | \hat{p} | \Psi_0 \rangle$, where $\hat{p}$ is the electric dipole operator. The circular components follow similar behaviour. The real circular birefringence (c) corresponds to the optical rotation and its change with wavelength is known as *optical rotatory dispersion* (ORD). The imaginary circular birefringence (d) corresponds to the difference in absorption of opposite circularly polarized states. This is called *circular dichroism* (CD) and is determined by the matrix elements of the type $\langle \Psi_1 | \hat{\alpha} | \Psi_0 \rangle$, where $\hat{\alpha}$ is the polarizability operator. Since $\hat{\alpha}$ is an even function, whereas $\hat{p}$ is an odd function, the selection rules for LD and CD are different, and each type of spectrum gives different information.

The link between optical rotation and crystal structure has been the subject of a great deal of work from the 18th century to date. Experimental methods for determining absolute chirality (Glazer & Stadnicka, 1989) of crystals only became routine in the late 1940s with the use of the X-ray anomalous dispersion effect,

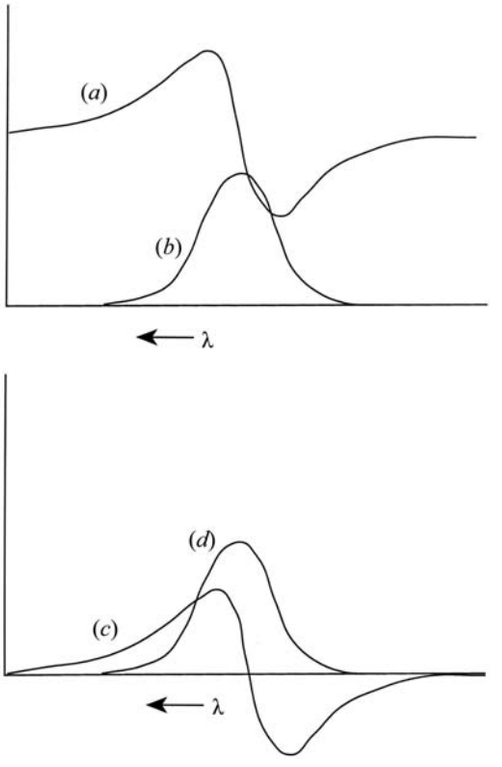

Fig. 1.6.5.2. Real and imaginary birefringence as a function of wavelength: (a) real linear; (b) imaginary linear; (c) real circular; (d) imaginary circular.

which made it possible to determine the absolute sense of the chiral nature of a crystal and then to link this to the sense of optical rotation. However, despite the preponderance of a great many complex theories, until recently, experimental evidence to support these theories has been fragmentary. It was shown by Glazer & Stadnicka (1986) that, at least for inorganic crystals, the problem lay in mistakes in the experiments or publications describing the experiments, rather than in the underlying theories. Once these errors are taken into account, it is possible to find a direct link between the chiral nature of the structure and the optical rotation, which appears to work in almost all cases. It has even been possible to produce a computer program *OPTACT* (Devarajan & Glazer, 1986; Glazer, 2002), using a polarizability theory based on earlier work by Born (1933), that is capable of calculating both the sign and magnitude of the effect with reasonable precision in many cases. *OPTACT* also calculates the refractive indices with good reliability.

1.6.5.2. *The dielectric tensor and spatial dispersion*

The relevant polarization term to consider here is

$$P_i^{\omega} = \omega_0 \chi_{ij\ell} \nabla_{\ell} E_j^{\omega}. \tag{1.6.5.3}$$

The important part of this expression is the use of the field gradient, which implies a variation of the electric field across the unit cell of the crystal rather than the assumption that **E** is everywhere constant. This variation in **E** is known as *spatial dispersion* (Agranovich & Ginzburg, 1984).

Assume propagation of a plane wave given by $\mathbf{E} = \mathbf{E_o} \exp(i\mathbf{k} \cdot \mathbf{r})$ through an optically active crystal. Substituting into the expression for the polarization gives

$$P_i^{\omega} = i\omega_0 \chi_{ij\ell} E_j^{\omega} k_{\ell}. \tag{1.6.5.4}$$

This term can now be treated as a perturbation to the dielectric tensor $\varepsilon_{ij}(\omega)$ to form the *effective* dielectric tensor $\varepsilon_{ij}(\omega, \mathbf{k})$:

$$\varepsilon_{ij}(\omega, \mathbf{k}) = \varepsilon_{ij}(\omega) + i\gamma_{ij\ell} k_{\ell}, \tag{1.6.5.5}$$

where $\gamma_{ij\ell}$ has been written for the susceptibility $\chi_{ij\ell}$ in order to distinguish it from the use of χ elsewhere. Note that this can be expressed more generally as a power-series expansion in the vector $\mathbf{k}$ (Agranovich & Ginzburg, 1984) to allow for a generalization to include all possible spatial dispersion effects:

$$\varepsilon_{ij}(\omega, \mathbf{k}) = \varepsilon_{ij}(\omega) + i\gamma_{ij\ell}(\omega)k_\ell + \alpha_{ij\ell m}(\omega)k_\ell k_m, \tag{1.6.5.6}$$

where the susceptibilities are in general themselves dependent on frequency.

1.6.5.3. *Symmetry of effective dielectric tensor*

To determine the symmetry constraints on the effective dielectric tensor, it should be recognized that the application of a real electric field $\mathbf{E}$ must lead to a real dielectric displacement $\mathbf{D}$. This therefore implies that one can write

$$\varepsilon_{ij}(\omega, \mathbf{k}) = \varepsilon^*_{ij}(-\omega^*, -\mathbf{k}^*)$$

or

$$\varepsilon_{ij}(\omega^*, \mathbf{k}^*) = \varepsilon^*_{ij}(-\omega, -\mathbf{k}). \tag{1.6.5.7}$$

Furthermore, in the absence of any absorptive processes, ε_{ij} must be Hermitian, that is

$$\varepsilon_{ij}(\omega, \mathbf{k}) = \varepsilon_{ji}(\omega, -\mathbf{k}). \tag{1.6.5.8}$$

This is fulfilled by the following symmetry constraints for the leading terms in the effective dielectric tensor:

$$\varepsilon_{ij}(\omega) = \varepsilon_{ji}(\omega); \quad \gamma_{ij\ell}(\omega) = -\gamma_{ji\ell}(\omega); \quad \alpha_{ij\ell m}(\omega) = \alpha_{ji\ell m}(\omega). \tag{1.6.5.9}$$

In a gyrotropic crystal, there must be at least one direction that is not equivalent to its opposite, and so such a crystal cannot have a centre of symmetry. (Only a noncentrosymmetric crystal can be gyrotropic. However, it is true to say that all non-gyrotropic crystals must be centrosymmetric.) Therefore, for a non-gyrotropic crystal,

$$\varepsilon_{ij}(\omega, \mathbf{k}) = \varepsilon_{ij}(\omega, -\mathbf{k}). \tag{1.6.5.10}$$

It follows therefore in such a case that

$$\gamma_{ij\ell}(\omega) = 0. \tag{1.6.5.11}$$

It is obvious then that the susceptibility $\gamma_{ij\ell}(\omega)$ has the required symmetry for gyration and that it forms an antisymmetric tensor of rank 3 (see Section 1.1.4.5.3 for the properties of antisymmetric tensors).

1.6.5.4. *Gyration tensor*

It is convenient to rewrite the effective dielectric expression in the following way (just keeping the first two terms):

$$\varepsilon_{ij}(\omega, \mathbf{k}) = \varepsilon_{ij}(\omega) + i\hat{e}_{ijm}g_{m\ell}k_l, \tag{1.6.5.12}$$

where $\hat{e}_{ijm}$ is a unit antisymmetric pseudotensor of rank 3 or permutation tensor ($\hat{e}_{123} = 1$, $\hat{e}_{213} = -1$, $\hat{e}_{112} = 0$ *etc.*; $\hat{e}_{ijm}$ is not affected by mirror reflection) and $g_{m\ell}$ represents a pseudotensor (*i.e.* axial tensor) of rank 2. One can then write further

$$\varepsilon_{ij}(\omega, \mathbf{k}) = \varepsilon_{ij}(\omega) + i\hat{e}_{ijm}G_m, \tag{1.6.5.13}$$

where $G_m = g_{m\ell}k_\ell$ is a component of a pseudovector (*i.e.* axial vector), known as the gyration vector. The formula for the dielectric displacement can then be expressed in the form

$$D_i = \varepsilon_o\varepsilon_{ij}(\omega, \mathbf{k})E_j = \varepsilon_o\big[\varepsilon_{ij}(\omega)E_j - i(\mathbf{G} \times \mathbf{E})_i\big]. \tag{1.6.5.14}$$

The operation $\mathbf{G} \times \mathbf{E}$ can also be represented by the product of an antisymmetric tensor $[G]$ with the vector $\mathbf{E}$:

$$\begin{pmatrix} 0 & G_{12} & G_{13} \\ -G_{12} & 0 & G_{23} \\ -G_{13} & -G_{23} & 0 \end{pmatrix}\begin{pmatrix} E_1 \\ E_2 \\ E_3 \end{pmatrix} = \begin{pmatrix} G_{12}E_2 + G_{13}E_3 \\ G_{23}E_3 - G_{12}E_1 \\ -G_{13}E_1 - G_{23}E_2 \end{pmatrix} = \begin{pmatrix} -G_3E_2 + G_2E_3 \\ -G_1E_3 + G_3E_1 \\ -G_2E_1 + G_1E_2 \end{pmatrix}, \tag{1.6.5.15}$$

where $-G_1 = G_{23} = -G_{32}$, $-G_2 = -G_{13} = G_{31}$ and $-G_3 = G_{12} = -G_{21}$. If $\hat{\mathbf{s}}$ is the unit vector in the propagation direction, then

$$\mathbf{G} = G\hat{\mathbf{s}} \tag{1.6.5.16}$$

and G represents the magnitude of the gyration vector. Thus,

$$\hat{\mathbf{s}} \cdot \mathbf{G} = \hat{\mathbf{s}} \cdot G\hat{\mathbf{s}} = G\hat{\mathbf{s}} \cdot \hat{\mathbf{s}} = G. \tag{1.6.5.17}$$

Consequently, if one knows the direction of propagation inside the crystal, the coefficient G can be calculated *via*

$$G = \hat{s}_1G_1 + \hat{s}_2G_2 + \hat{s}_3G_3 \tag{1.6.5.18}$$

and then the optical *rotatory power* is defined as

$$\rho = \frac{\pi G}{\lambda n}, \tag{1.6.5.19}$$

where ρ is the angle of rotation in degrees per millimetre. According to the way in which the sign of G has been defined here, a positive value of ρ means dextrorotation and a negative value means laevorotation.

There is a possibility of confusion here in terminology with respect to the term 'gyration tensor'. It is seen that there exists an antisymmetric tensor $[G]$: this is sometimes referred to as the gyration tensor. However, returning to equation (1.6.5.12), it is the pseudotensor given by $g_{m\ell}$ that is more often described as the gyration tensor. The difference between them is really one of emphasis. The $[G]$ tensor refers to the polarization directions of the wave, whereas the g tensor is referred to the direction of wave propagation. Thus, for example, G_{23} refers to a wave whose polarization lies in the x_2x_3 plane, and so propagates in the x_1 direction, according to the axial gyration vector component $-G_1$. The gyration is equally described by the tensor component g_{11}. Being an axial tensor, g_{11} corresponds to a wave travelling along x_1, along which direction one observes a rotation in the x_2x_3 plane.

Although g is in general an antisymmetric tensor, since it is only the scalar products $g_{m\ell}\hat{s}_m\hat{s}_\ell$ that are important in determining the rotation of the plane of polarization, the components of $\mathbf{D}$, and hence the refractive index behaviour, are independent of the antisymmetric part of $g_{m\ell}$. It is thus possible to construct a table of tensor invariances for the symmetric part of the gyration tensor with regard to the possible symmetry classes of a crystal (Table 1.6.5.1). For a discussion of the importance of the antisymmetric terms, see Agranovich & Ginzburg (1984).

1.6.5.5. *Optical rotation along the optic axis of a uniaxial crystal*

Consider a uniaxial crystal such as quartz, crystallizing in point group 32. In this case, the only dielectric tensor terms (for the effect of symmetry, see Section 1.1.4.10) are $\varepsilon_{11} = \varepsilon_{22} \neq \varepsilon_{33}$, with the off-diagonal terms equal to zero. The equations for the dielectric displacements along the three coordinate axes x_1, x_2 and x_3 are then given, according to equations (1.6.5.14) and (1.6.5.15), by

Table 1.6.5.1. *Symmetry constraints (see Section 1.1.4.10) on the gyration tensor g_{ij}*

All g_{ij} components are zero for the centrosymmetric point groups plus $4mm$, $\bar{4}3m$, $3m$, $6mm$, $\bar{6}$ and $\bar{6}m2$.

Triclinic	Monoclinic		Orthorhombic
Point group 1	Point group 2 ($2 \parallel x_2$)	Point group m ($m \perp x_2$)	Point group 222
$\begin{pmatrix} g_{11} & g_{12} & g_{13} \\ g_{12} & g_{22} & g_{23} \\ g_{13} & g_{23} & g_{33} \end{pmatrix}$	$\begin{pmatrix} g_{11} & 0 & g_{13} \\ 0 & g_{22} & 0 \\ g_{13} & 0 & g_{33} \end{pmatrix}$	$\begin{pmatrix} 0 & g_{12} & 0 \\ g_{12} & 0 & g_{23} \\ 0 & g_{23} & 0 \end{pmatrix}$	$\begin{pmatrix} g_{11} & 0 & 0 \\ 0 & g_{22} & 0 \\ 0 & 0 & g_{33} \end{pmatrix}$
	Point group 2 ($2 \parallel x_3$)	Point group m ($m \perp x_3$)	Point group $mm2$
	$\begin{pmatrix} g_{11} & g_{12} & 0 \\ g_{12} & g_{22} & 0 \\ 0 & 0 & g_{33} \end{pmatrix}$	$\begin{pmatrix} 0 & & g_{13} \\ & 0 & g_{23} \\ g_{13} & g_{23} & 0 \end{pmatrix}$	$\begin{pmatrix} 0 & g_{12} & 0 \\ g_{12} & 0 & 0 \\ 0 & 0 & 0 \end{pmatrix}$

Tetragonal		Trigonal and hexagonal	Cubic and isotropic
Point groups 4, 422	Point group $\bar{4}$	Point groups 3, 32, 6, 622	Point groups 432, 23
$\begin{pmatrix} g_{11} & 0 & 0 \\ 0 & g_{11} & 0 \\ 0 & 0 & g_{33} \end{pmatrix}$	$\begin{pmatrix} g_{11} & g_{12} & 0 \\ g_{12} & -g_{11} & 0 \\ 0 & 0 & 0 \end{pmatrix}$	$\begin{pmatrix} g_{11} & 0 & 0 \\ 0 & g_{11} & 0 \\ 0 & 0 & g_{33} \end{pmatrix}$	$\begin{pmatrix} g_{11} & 0 & 0 \\ 0 & g_{11} & 0 \\ 0 & 0 & g_{11} \end{pmatrix}$
Point group $\bar{4}2m$			Isotropic, no centre of symmetry
$\begin{pmatrix} g_{11} & 0 & 0 \\ 0 & -g_{11} & 0 \\ 0 & 0 & 0 \end{pmatrix}$			$\begin{pmatrix} g_{11} & 0 & 0 \\ 0 & g_{11} & 0 \\ 0 & 0 & g_{11} \end{pmatrix}$

$$\begin{aligned} D_1 &= \varepsilon_o \varepsilon_{11} E_1 - i\varepsilon_o \big[G_{12} E_2 + G_{13} E_3\big] \\ D_2 &= \varepsilon_o \varepsilon_{22} E_2 - i\varepsilon_o \big[G_{23} E_3 - G_{21} E_1\big] \\ D_3 &= \varepsilon_o \varepsilon_{33} E_3 - i\varepsilon_o \big[G_{31} E_1 - G_{32} E_2\big]. \end{aligned} \tag{1.6.5.20}$$

If the light is taken to propagate along x_3, the optic axis, the fundamental optics equation (1.6.3.14) is expressed as

$$\begin{aligned} &\begin{pmatrix} \varepsilon_{11} & -iG_{12} & -iG_{13} \\ iG_{12} & \varepsilon_{11} & -iG_{23} \\ iG_{13} & iG_{23} & \varepsilon_{33} + n^2 \end{pmatrix} \begin{pmatrix} E_1 \\ E_2 \\ E_3 \end{pmatrix} \\ &= \begin{pmatrix} n^2 & 0 & 0 \\ 0 & n^2 & 0 \\ 0 & 0 & n^2 \end{pmatrix} \begin{pmatrix} E_1 \\ E_2 \\ E_3 \end{pmatrix}. \end{aligned} \tag{1.6.5.21}$$

As usual, the longitudinal solution given by

$$iG_{13} E_1 + iG_{23} E_2 + \varepsilon_{33} E_3 = 0 \tag{1.6.5.22}$$

can be ignored, as one normally deals with a transverse electric field in the normal case of propagating light. For a non-trivial solution, then,

$$\begin{vmatrix} \varepsilon_{11} - n^2 & -iG_{12} \\ iG_{12} & \varepsilon_{11} - n^2 \end{vmatrix} = 0, \tag{1.6.5.23}$$

which gives

$$n^2 = \varepsilon_{11} \pm G_{12}. \tag{1.6.5.24}$$

This results in two eigenvalue solutions, n_1 and n_2, from which one has

$$(n_1 - n_2)(n_1 + n_2) = 2G_{12} = -2G_3 \tag{1.6.5.25}$$

and thus

$$n_1 - n_2 = \frac{G_{12}}{\bar{n}} = -\frac{G_3}{\bar{n}}. \tag{1.6.5.26}$$

The optical rotatory power (1.6.5.19) is then given by

$$\rho = \frac{\pi G_3}{\lambda \bar{n}} = \frac{\pi (n_2 - n_1)}{\lambda}. \tag{1.6.5.27}$$

Note that in order to be consistent with the definition of rotatory power used here, $n_2 > n_1$ for a dextrorotatory solution. This implies that n_2 should be identified with n_L and n_1 with n_R. To check this, find the eigenvectors corresponding to the two solutions (1.6.5.24).

For $n_1^2 = \varepsilon_{11} - G_3$, the following matrix is found from (1.6.5.21):

$$\begin{pmatrix} G_3 & iG_3 \\ -iG_3 & G_3 \end{pmatrix} = 0, \tag{1.6.5.28}$$

giving the Jones matrix

$$(1/2^{1/2}) \begin{pmatrix} 1 \\ -i \end{pmatrix} = 0. \tag{1.6.5.29}$$

This corresponds to a right-circularly polarized wave. It should be noted that there is confusion in the optics textbooks over the Jones matrices for circular polarizations. Jones (1948) writes a right-circular wave as

$$\begin{pmatrix} 1 \\ i \end{pmatrix},$$

but this is for a definition of right-circularly polarized light as that for which an instantaneous picture of the space distribution of its electric vector describes a right spiral. The modern usage is to define the sense of circular polarization through the time variation of the electric vector in a given plane as seen by an observer

looking towards the source of the light. This reverses the definition given by Jones.

For $n_2^2 = \varepsilon_{11} + G_3$, the following matrix is found:

$$\begin{pmatrix} -G_3 & iG_3 \\ -iG_3 & -G_3 \end{pmatrix} = 0, \tag{1.6.5.30}$$

giving

$$(1/2^{1/2})\begin{pmatrix} 1 \\ i \end{pmatrix} = 0. \tag{1.6.5.31}$$

This corresponds to a left-circularly polarized wave. Therefore it is proved that the optical rotation arises from a competition between two circularly polarized waves and that in equation (1.6.5.26) $n_1 = n_R$ and $n_2 = n_L$, the refractive indices for right- and left-circularly polarized light, respectively. Note that Fresnel's original idea of counter-rotating circular polarizations fits nicely with the eigenvectors rigorously determined in (1.6.5.29) and (1.6.5.31). Thus

$$\rho = \frac{\pi(n_L - n_R)}{\lambda}. \tag{1.6.5.32}$$

Finally, for light propagating along x_3 in quartz, one can write the direction of the wave normal as

$$\hat{s}_1 = 0; \quad \hat{s}_2 = 0; \quad \hat{s}_3 = 1 \tag{1.6.5.33}$$

and then the gyration vector is given by

$$G = g_{i3}\hat{s}_i\hat{s}_3 = g_{13} + g_{23} + g_{33} = g_{33} \tag{1.6.5.34}$$

as $g_{12} = g_{23} = 0$ in point group 32. Thus from (1.6.5.26) it is seen that

$$g_{33} = G_3 = -G_{12}, \tag{1.6.5.35}$$

thus linking one of the components of the gyration tensor $g_{m\ell}$ with a component of the gyration vector **G** and a tensor component of $[G]$.

1.6.5.6. *Optical rotation perpendicular to the optic axis of a uniaxial crystal*

The magnitude of circular birefringence is typically about 10^{-4} times smaller than that of linear birefringence. For this reason, optical rotation has usually been observed only in directions where the linear birefringence is absent, such as in optic axial directions. However, it has been clear for some time that optical rotation also exists in other directions and that with specialized techniques it is even possible to measure it. The techniques (Moxon & Renshaw, 1990; Moxon *et al.*, 1991) are complex and require very precise measuring capabilities, and therefore are generally not commonly available.

Probably the best known case where optical rotation has been measured in a linearly birefringent section is that of quartz. It has been seen that it is easy to measure the rotation along the optic axial direction, since this is the direction along which the crystal looks isotropic. Szivessy & Münster (1934) measured the rotation in a direction perpendicular to the optic axis and found that its magnitude was smaller and opposite in sign to that along the optic axis of the same crystal.

To see the relationship between the linear and circular birefringences, consider light travelling along x_1 in quartz. The fundamental equation (1.6.3.14) then becomes

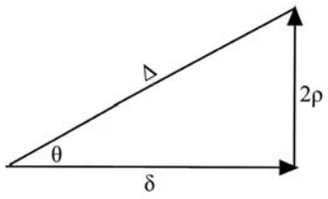

Fig. 1.6.5.3. The principle of superposition.

$$\begin{pmatrix} \varepsilon_{11} - n^2 & -iG_{12} & -iG_{13} \\ iG_{12} & \varepsilon_{11} & -iG_{23} \\ iG_{13} & iG_{23} & \varepsilon_{33} \end{pmatrix}\begin{pmatrix} E_1 \\ E_2 \\ E_3 \end{pmatrix} = \begin{pmatrix} n^2 & 0 & 0 \\ 0 & n^2 & 0 \\ 0 & 0 & n^2 \end{pmatrix}\begin{pmatrix} E_1 \\ E_2 \\ E_3 \end{pmatrix}. \tag{1.6.5.36}$$

Solving for the non-trivial transverse solutions

$$\begin{vmatrix} \varepsilon_{11} - n^2 & -iG_{23} \\ iG_{23} & \varepsilon_{33} - n^2 \end{vmatrix} = 0 \tag{1.6.5.37}$$

and then

$$n^4 - n^2(\varepsilon_{11} + \varepsilon_{33}) + \varepsilon_{11}\varepsilon_{33} - G_{23}^2 = 0. \tag{1.6.5.38}$$

Finding the roots of this equation considered as a quadratic in n^2, the following birefringence is obtained:

$$n_1 - n_2 = \left[(n_o - n_e)^2 + (G_{23}^2/\bar{n}^2)\right]^{1/2}. \tag{1.6.5.39}$$

The eigenvectors for the two solutions n_1 and n_2 can easily be shown to correspond to elliptical polarizations. Notice that in equation (1.6.5.39), two refractive-index solutions are obtained whose difference depends on two terms, one with respect to the linear birefringence $n_o - n_e$ and the other to the circular birefringence represented by the gyration component $G_{23} = -G_1$. The refractive-index difference $n_1 - n_2$ gives rise to a phase shift between the two elliptically polarized components of the light, given by

$$\Delta = (2\pi/\lambda)(n_1 - n_2), \tag{1.6.5.40}$$

from which

$$\Delta^2 = (4\pi^2/\lambda^2)\left[(n_o - n_e)^2 + (G_{23}^2/\bar{n}^2)\right] = \delta^2 + (2\rho)^2, \tag{1.6.5.41}$$

where

$$\delta = \frac{2\pi}{\lambda}(n_o - n_e) \quad \text{and} \quad \rho = \frac{-\pi G_{23}}{\lambda\bar{n}} = \frac{-\pi G_1}{\lambda\bar{n}}. \tag{1.6.5.42}$$

δ is the phase difference when there is no optical rotation and 2ρ is the phase difference corresponding to a normal optical rotation ρ when there is no linear birefringence. (1.6.5.41) shows that the linear and circular terms simply add, and this is known as the *principle of superposition*.

This reveals that an elliptical polarization is created by the simple vector addition of a linearly polarized wave to a circularly polarized wave, as indicated in Fig. 1.6.5.3. From this, the ellipticity κ of the polarization is given by

$$\kappa = \tan(\tfrac{1}{2}\theta), \tag{1.6.5.43}$$

where

$$\tan\theta = \frac{2\rho}{\delta}. \tag{1.6.5.44}$$

Table 1.6.6.1. *Symmetry constraints (see Section 1.1.4.10) on the linear electro-optic tensor r_{ij} (contracted notation)*

Triclinic	Monoclinic		Orthorhombic
Point group 1	Point group 2 ($2 \parallel x_2$)	Point group m ($m \perp x_2$)	Point group 222
$\begin{pmatrix} r_{11} & r_{12} & r_{13} \\ r_{21} & r_{22} & r_{23} \\ r_{31} & r_{32} & r_{33} \\ r_{41} & r_{42} & r_{43} \\ r_{51} & r_{52} & r_{53} \\ r_{61} & r_{62} & r_{63} \end{pmatrix}$	$\begin{pmatrix} 0 & r_{12} & 0 \\ 0 & r_{22} & 0 \\ 0 & r_{32} & 0 \\ r_{41} & 0 & r_{43} \\ 0 & r_{52} & 0 \\ r_{61} & 0 & r_{63} \end{pmatrix}$	$\begin{pmatrix} r_{11} & 0 & r_{13} \\ r_{21} & 0 & r_{23} \\ r_{31} & 0 & r_{33} \\ 0 & r_{42} & 0 \\ r_{51} & 0 & r_{53} \\ 0 & r_{62} & 0 \end{pmatrix}$	$\begin{pmatrix} 0 & 0 & 0 \\ 0 & 0 & 0 \\ 0 & 0 & 0 \\ r_{41} & 0 & 0 \\ 0 & r_{52} & 0 \\ 0 & 0 & r_{63} \end{pmatrix}$
	Point group 2 ($2 \parallel x_3$)	Point group m ($m \perp x_3$)	Point group $mm2$
	$\begin{pmatrix} 0 & 0 & r_{13} \\ 0 & 0 & r_{23} \\ 0 & 0 & r_{33} \\ r_{41} & r_{42} & 0 \\ r_{51} & r_{52} & 0 \\ 0 & 0 & r_{63} \end{pmatrix}$	$\begin{pmatrix} r_{11} & r_{12} & 0 \\ r_{21} & r_{22} & 0 \\ r_{31} & r_{32} & 0 \\ 0 & 0 & r_{43} \\ 0 & 0 & r_{53} \\ r_{61} & r_{62} & 0 \end{pmatrix}$	$\begin{pmatrix} 0 & 0 & r_{13} \\ 0 & 0 & r_{23} \\ 0 & 0 & r_{33} \\ 0 & r_{42} & 0 \\ r_{51} & 0 & 0 \\ 0 & 0 & 0 \end{pmatrix}$

Tetragonal		Trigonal	
Point group 4	Point group $\bar{4}$	Point group 3	Point group 32
$\begin{pmatrix} 0 & 0 & r_{13} \\ 0 & 0 & r_{13} \\ 0 & 0 & r_{33} \\ r_{41} & r_{51} & 0 \\ r_{51} & -r_{41} & 0 \\ 0 & 0 & 0 \end{pmatrix}$	$\begin{pmatrix} 0 & 0 & r_{13} \\ 0 & 0 & -r_{13} \\ 0 & 0 & 0 \\ r_{41} & -r_{51} & 0 \\ r_{51} & r_{41} & 0 \\ 0 & 0 & r_{63} \end{pmatrix}$	$\begin{pmatrix} r_{11} & -r_{22} & r_{13} \\ -r_{11} & r_{22} & r_{13} \\ 0 & 0 & r_{33} \\ r_{41} & r_{51} & 0 \\ r_{51} & -r_{41} & 0 \\ -r_{22} & -r_{11} & 0 \end{pmatrix}$	$\begin{pmatrix} r_{11} & 0 & 0 \\ -r_{11} & 0 & 0 \\ 0 & 0 & 0 \\ r_{41} & 0 & 0 \\ 0 & -r_{41} & 0 \\ 0 & -r_{11} & 0 \end{pmatrix}$
Point group $\bar{4}2m$	Point group 422	Point group $3m1$ ($m \perp x_1$)	Point group $31m$ ($m \perp x_2$)
$\begin{pmatrix} 0 & 0 & 0 \\ 0 & 0 & 0 \\ 0 & 0 & 0 \\ r_{41} & & 0 \\ & r_{41} & 0 \\ 0 & 0 & r_{63} \end{pmatrix}$	$\begin{pmatrix} 0 & 0 & 0 \\ 0 & 0 & 0 \\ 0 & 0 & 0 \\ r_{41} & 0 & 0 \\ 0 & -r_{41} & 0 \\ 0 & 0 & 0 \end{pmatrix}$	$\begin{pmatrix} 0 & -r_{22} & r_{13} \\ 0 & r_{22} & r_{13} \\ 0 & 0 & r_{33} \\ 0 & r_{51} & 0 \\ r_{51} & 0 & 0 \\ -r_{22} & 0 & 0 \end{pmatrix}$	$\begin{pmatrix} r_{11} & 0 & r_{13} \\ -r_{11} & 0 & r_{13} \\ 0 & 0 & r_{33} \\ 0 & r_{51} & 0 \\ r_{51} & 0 & 0 \\ 0 & -r_{11} & 0 \end{pmatrix}$
Point group $4mm$			
$\begin{pmatrix} 0 & 0 & r_{13} \\ 0 & 0 & r_{13} \\ 0 & 0 & r_{33} \\ 0 & r_{51} & 0 \\ r_{51} & 0 & 0 \\ 0 & 0 & 0 \end{pmatrix}$			

Hexagonal			Cubic
Point group 6	Point group $6mm$	Point group 622	Point groups $\bar{4}3m$, 23
$\begin{pmatrix} 0 & 0 & r_{13} \\ 0 & 0 & r_{13} \\ 0 & 0 & r_{33} \\ r_{41} & r_{51} & 0 \\ r_{51} & -r_{41} & 0 \\ 0 & 0 & 0 \end{pmatrix}$	$\begin{pmatrix} 0 & 0 & r_{13} \\ 0 & 0 & r_{13} \\ 0 & 0 & r_{33} \\ 0 & r_{51} & 0 \\ r_{51} & 0 & 0 \\ 0 & 0 & 0 \end{pmatrix}$	$\begin{pmatrix} 0 & 0 & 0 \\ 0 & 0 & 0 \\ 0 & 0 & 0 \\ r_{41} & 0 & 0 \\ 0 & -r_{41} & 0 \\ 0 & 0 & 0 \end{pmatrix}$	$\begin{pmatrix} 0 & 0 & 0 \\ 0 & 0 & 0 \\ 0 & 0 & 0 \\ r_{41} & 0 & 0 \\ 0 & r_{41} & 0 \\ 0 & 0 & r_{41} \end{pmatrix}$
Point group $\bar{6}$	Point group $\bar{6}m2$ ($m \perp x_1$)	Point group $\bar{6}2m$ ($m \perp x_2$)	Point group 432
$\begin{pmatrix} r_{11} & -r_{22} & 0 \\ -r_{11} & r_{22} & 0 \\ 0 & 0 & 0 \\ 0 & 0 & 0 \\ 0 & 0 & 0 \\ -r_{22} & -r_{11} & 0 \end{pmatrix}$	$\begin{pmatrix} 0 & -r_{22} & 0 \\ 0 & r_{22} & 0 \\ 0 & 0 & 0 \\ 0 & 0 & 0 \\ 0 & 0 & 0 \\ -r_{22} & 0 & 0 \end{pmatrix}$	$\begin{pmatrix} r_{11} & 0 & 0 \\ -r_{11} & 0 & 0 \\ 0 & 0 & 0 \\ 0 & 0 & 0 \\ 0 & 0 & 0 \\ 0 & -r_{11} & 0 \end{pmatrix}$	$\begin{pmatrix} 0 & 0 & 0 \\ 0 & 0 & 0 \\ 0 & 0 & 0 \\ 0 & 0 & 0 \\ 0 & 0 & 0 \\ 0 & 0 & 0 \end{pmatrix}$

Thus

$$\tan\theta = \frac{G_1}{\bar{n}(n_o - n_e)} = \frac{g_{11}}{\bar{n}(n_o - n_e)}. \qquad (1.6.5.45)$$

Generally speaking, the ellipticity is extremely small and difficult to measure (Moxon & Renshaw, 1990). In right-handed quartz (right-handed with respect to optical rotation observed along the c axis), $n_o = 1.544$, $n_e = 1.553$, $g_{11} = g_{22} = -5.82 \times 10^{-5}$ and $g_{33} = 12.96 \times 10^{-5}$ measured at $\lambda = 5100$ Å. Since the c axis is also the optic axis, $\delta = 0$ for the (0001) plane, and thus $\kappa = 1$ for this section [equations (1.6.5.44) and (1.6.5.43)]. This value of $\kappa = 1$ means that the two waves are circular (see Section 1.6.5.5), *i.e.* there is no linear birefringence, only a pure rotation. In this direction, the gyration g_{33} means a rotation of $\rho = 29.5^\circ\ \text{mm}^{-1}$ [using equation (1.6.5.27)]. In a direction normal to the optic axis, from equation (1.6.5.40) one finds $\rho = -13.3^\circ\ \text{mm}^{-1}$. However, in this direction, the crystal appears linearly birefringent with $\delta = 110.88\ \text{mm}^{-1}$ [equation (1.6.5.42)]. Thus the ellipticity $\kappa = -0.00209$, as calculated from equations (1.6.5.44) and (1.6.5.43). In other words, the two waves are very slightly elliptical, and the sense of rotation of the two ellipses is reversed. Because of the change in sign of the gyration coefficients, it is found that at an angle of $56^\circ\ 10'$ down from the optic axis $\kappa = 0$, meaning that waves travelling along this direction show no optical rotation, only linear birefringence.

1.6.6. Linear electro-optic effect

The linear electro-optic effect, given by $P_i^\omega = \varepsilon_o \chi_{ijk} E_j^\omega E_k^0$, is conventionally expressed in terms of the change in dielectric impermeability caused by imposition of a static electric field on the crystal. Thus one may write the linear electro-optic effect as

$$\Delta\eta_{ij} = r_{ijk} E_k^0, \qquad (1.6.6.1)$$

where the coefficients r_{ijk} form the so-called *linear electro-optic tensor*. These have identical symmetry with the piezoelectric tensor and so obey the same rules (see Table 1.6.6.1). Like the piezoelectric tensor, there is a maximum of 18 independent coefficients (triclinic case) (see Section 1.1.4.10.3). However, unlike in piezoelectricity, in using the Voigt contracted notation there are two major differences:

(1) In writing the electro-optic tensor components as r_{ij}, the first suffix refers to the column number and the second suffix is the row number.

(2) There are no factors of 1/2 or 2.

Typical values of linear electro-optic coefficients are around $10^{-12}\ \text{mV}^{-1}$.

1.6.6.1. *Primary and secondary effects*

In considering the electro-optic effect, it is necessary to bear in mind that, in addition to the primary effect of changing the refractive index, the applied electric field may also cause a strain in the crystal *via* the converse piezoelectric effect, and this can then change the refractive index, as a secondary effect, through the elasto-optic effect. Both these effects, which are of comparable magnitude in practice, will occur if the crystal is free. However, if the crystal is mechanically clamped, it is not possible to induce any strain, and in this case therefore only the primary electro-optic effect is seen. In practice, the free and clamped behaviour can be investigated by measuring the linear birefringence when applying electric fields of varying frequencies. When the electric field is static or of low frequency, the effect is measured at constant stress, so that both primary and secondary effects are measured together. For electric fields at frequencies above the natural mechanical resonance of the crystal, the strains are very small, and in this case only the primary effect is measured.

1.6.6.2. *Example of $LiNbO_3$*

In order to understand how tensors can be used in calculating the optical changes induced by an applied electric field, it is instructive to take a particular example and work out the change in refractive index for a given electric field. $LiNbO_3$ is the most widely used electro-optic material in industry and so this forms a useful example for calculation purposes. This material crystallizes in point group $3m$, for which the electro-optic tensor has the form (for the effect of symmetry, see Section 1.1.4.10) (with x_1 perpendicular to m)

$$\begin{pmatrix} 0 & -r_{22} & r_{13} \\ 0 & r_{22} & r_{13} \\ 0 & 0 & r_{33} \\ 0 & r_{51} & 0 \\ r_{51} & 0 & 0 \\ -r_{22} & 0 & 0 \end{pmatrix}, \qquad (1.6.6.2)$$

with $r_{13} = 9.6$, $r_{22} = 6.8$, $r_{33} = 30.9$ and $r_{51} = 32.5 \times 10^{-12}\ \text{mV}^{-1}$, under the normal measuring conditions where the crystal is unclamped.

Calculation using dielectric impermeability tensor. Suppose, for example, a static electric field E_3^0 is imposed along the x_3 axis. One can then write

$$\begin{pmatrix} \Delta\eta_1 \\ \Delta\eta_2 \\ \Delta\eta_3 \\ \Delta\eta_4 \\ \Delta\eta_5 \\ \Delta\eta_6 \end{pmatrix} = \begin{pmatrix} 0 & -r_{22} & r_{13} \\ 0 & r_{22} & r_{13} \\ 0 & 0 & r_{33} \\ 0 & r_{51} & 0 \\ r_{51} & 0 & 0 \\ -r_{22} & 0 & 0 \end{pmatrix} \begin{pmatrix} 0 \\ 0 \\ E_3^0 \end{pmatrix} = \begin{pmatrix} r_{13}E_3^0 \\ r_{13}E_3^0 \\ r_{33}E_3^0 \\ 0 \\ 0 \\ 0 \end{pmatrix}. \qquad (1.6.6.3)$$

Thus

$$\begin{aligned} \Delta\eta_1 &= r_{13}E^0 = \Delta\eta_2 \\ \Delta\eta_3 &= r_{33}E^0 \\ \Delta\eta_4 &= \Delta\eta_5 = \Delta\eta_6 = 0. \end{aligned} \qquad (1.6.6.4)$$

Since the original indicatrix of $LiNbO_3$ before application of the field is uniaxial,

$$\begin{aligned} \eta_1 &= \frac{1}{n_o^2} = \eta_2 \\ \eta_3 &= \frac{1}{n_e^2}, \end{aligned} \qquad (1.6.6.5)$$

and so differentiating, the following are obtained:

$$\begin{aligned} \Delta\eta_1 &= \Delta\eta_2 = -\frac{2}{n_o^3}\Delta n_o \\ \Delta\eta_3 &= -\frac{2}{n_e^3}\Delta n_e. \end{aligned} \qquad (1.6.6.6)$$

Thus, the induced changes in refractive index are given by

$$\begin{aligned} \Delta n_1 &= \Delta n_2 = -\frac{n_o^3}{2} r_{13} E_3^0 \\ \Delta n_3 &= -\frac{n_e^3}{2} r_{33} E_3^0. \end{aligned} \qquad (1.6.6.7)$$

It can be seen from this that the effect is simply to change the refractive indices by deforming the indicatrix, but maintain the uniaxial symmetry of the crystal. Note that if light is now propagated along, say, x_1, the observed linear birefringence is given by

$$(n_e - n_o) - \tfrac{1}{2}(n_e^3 r_{33} - n_o^3 r_{13}) E_3^0. \qquad (1.6.6.8)$$